Frequency Generation and Solitonic Decay in ThreeWave Interactions

Fabio Baronio, Matteo Conforti, Marco Andreana, Vincent Couderc, Costantino de Angelis, Stefan Wabnitz, Alain Barthélémy, Antonio Degasperis

Frequency Generation and Solitonic Decay in Three Wave Interactions

Fabio Baronio,[1] Matteo Conforti,[1] Marco Andreana,[2] Vincent Couderc,[2] Costantino De Angelis,[1] Stefan Wabnitz, [1] Alain Barthélémy,[2] Antonio Degasperis[3]

[1]*CNISM, Dipartimento di Elettronica per l'Automazione, Università di Brescia, Via Branze 38, 25123 Brescia, Italy*

[2] *XLIM Research Institute, Centre National de la Recherche Scientifique, University of Limoges, Av. Albert Thomas 123, 87060, Limoges, France*

[3]*Dipartimento di Fisica and Istituto Nazionale di Fisica Nucleare, "Sapienza" Università di Roma, P.le A. Moro 2, 00185 Roma, Italy*

*fabio.baronio@ing.unibs.it

Abstract: We consider experimentally three–wave resonant nonlinear interactions of fields propagating in nonlinear media. We investigate the spatial dynamics of two diffractionless beams at frequency ω_1, ω_2 which mix to generate a field at the sum frequency ω_3. If the generated field at ω_3 can sustain a soliton, it decays into solitons at ω_1, ω_2. We report the experimental evidence of the transition from steady frequency wave generation to solitonic decay in nonlinear optics.

OCIS codes: (190.5530) Pulse propagation and solitons; (190.2620) Frequency conversion; (190.4410) Nonlinear optics, parametric processes.

References and links

1. D.J. Kaup, A. Reiman, A. Bers, "Space-time evolution of nonlinear three-wave interactions. I. Interaction in a homogeneous medium," Rev. Mod. Phys. **51,** 275–309 (1979).
2. B. Kim, J. Blake, H. Engan, H. Shaw, "All-fiber acousto-optic frequency shifter," Opt. Lett. **11,** 389–391 (1986).
3. P. Russel, D. Culverhouse, and F. Farahi, "Theory of Forward Stimulated Brillouin Scattering in Dual-Mode Single-Core Fibers," IEEE J. Quantum Electron. **27,** 836–842 (1991).
4. E. Ibragimov, and A. Struthers, "Second harmonic pulse compression in the soliton regime," Opt. Lett. **21,** 1582–1584 (1996).
5. M. Conforti, F. Baronio, A. Degasperis, and S. Wabnitz, "Parametric frequency conversion of short optical pulses controlled by a CW background," Opt. Express **15,** 12246–12251 (2007).
6. F. Baronio, M. Conforti, A. Degasperis, and S. Wabnitz, "Three-wave trapponic solitons for tunable high-repetition rate pulse train generation ," IEEE J. Quantum Electron. **44,** 542–546 (2008).
7. A. Hasegawa, *Plasma Instabilities and Nonlinear Effects* (Springer-Verlag, Berlin, 2001).
8. Y. Tsidulko, V. Malkin, and N. Fisch, "Suppression of Superluminous Precursors in High-Power Backward Raman Amplifiers," Phys. Rev. Lett. **88,** 235004 (2002).
9. W. Cheng, Y. Avitzour, Y. Ping, S. Suckewer, N. Fisch, M. Hur, and J. Wurtele, "Reaching the Nonlinear Regime of Raman Amplification of Ultrashort Laser Pulses," Phys. Rev. Lett. **94,** 045003 (2005).
10. A. Craik, *Wave Interactions and Fluid Flows* (Cambridge Univ. Press, Cambridge, 1985).
11. K. Lamb, "Tidally generated near-resonant internal wave triads at shelf break," Geophys. Res. Lett. **34,** L18607 (2007).
12. L. Svaasand, "Interaction between elastic surface waves in piezoelectric materials," Appl. Phys. Lett. **15,** 300–302 (1969).
13. Y. N. Karamzin, and A. P. Sukhorukov "Nonlinear interaction of diffracted light beams in a medium with quadratic nonlinearity: mutual focusing of beams and limitation on the efficiency of optical frequency converters," JEPT Lett. **20,** 339–344 (1974).
14. A. Buryak, P. Di Trapani, D. Skryabin, and S. Trillo "Optical solitons due to quadratic nonlinearities: from basic physics to futuristic applications ," Phys. Rep. **370,** 63–235 (2002).

#112662 - $15.00 USD Received 12 Jun 2009; accepted 18 Jun 2009; published 27 Jul 2009

15. V. E. Zakharov, and S. V. Manakov, "Resonant interaction of wave packets in nonlinear media," Jept. Lett. **18,** 243–245 (1973).
16. K. Nozaki, and T. Taniuti, "Propagation of solitary pulses in interactions of plasma waves," J. Phys. Soc. Jpn. **34,** 796–800 (1973).
17. V. E. Zakharov, *What is integrability?* (Springer Verlag, Berlin, 1991).
18. V. E. Zakharov, S. V. Manakov, S. P. Novikov, and L. P. Pitajevski, *The Theory of Solitons: The Inverse Problem Method*, (Nauka, Moskow, 1980).

1. Introduction

Three–wave resonant interaction (TWRI) is a universal model that recurs in various branches of science, such as plasma physics, optics, fluid dynamics and acoustics, as it describes the mixing of waves with different frequencies in weakly nonlinear and dispersive media [1]. In general, TWRI is typically encountered in the description of any conservative nonlinear medium where the nonlinear dynamics can be considered as a perturbation of the linear wave solution, the lowest–order nonlinearity is quadratic in the field amplitudes and the three–wave resonance can be satisfied. Indeed TWRI is the lowest–order nonlinear effect for a system approximately described by a linear superposition of discrete (i.e. quasi monochromatic) waves. TWRI has been extensively studied alongside with the development of nonlinear optics, since it describes stimulated Raman and Brillouin scattering, parametric amplification, frequency conversion [2, 3, 4, 5, 6]. In the domain of plasma physics, TWRI applies to the saturation of parametric decay instabilities, nonlinear collisions of large–amplitude wave packets, radio frequency heating, and laser–plasma interactions [7, 8, 9]. TWRIs have also been studied in the context of interactions of water waves [10, 11], interactions of bulk acoustic waves and surface acoustic waves [12]. In recent years, soliton waves in quadratic materials have been the subject of an intense renewal of interest from both theoretical and experimental viewpoints because of their particle–like behavior, which enables the coherent energy transport and processing. Two types of soliton waves that were both predicted in the early 1970s have been studied. On the one hand, one finds solitary waves that result from a balance between nonlinearity and dispersion (or diffraction) as first predicted by Karamzin and Sukhorukov [13]. This type of soliton waves have been intensively investigated experimentally over the past few years [14]. On the other hand, quadratic media were shown to support soliton waves that result from energy exchanges between dispersionless (or diffractionless) waves of different velocities as first predicted by Zakharov and Manakov [15] and Nozaki [16].

Here we investigate the TWRI dynamics of two input beams at frequencies ω_1 and ω_2 which mix to generate a field at the sum frequency ω_3, in absence of diffraction. Depending on the input intensities, three different regimes exist. Linear regime: the beams at frequency ω_1 and ω_2 don't interact. Frequency conversion: the beams at frequencies ω_1 and ω_2 interact and generate a steady field at the sum frequency ω_3. Solitonic regime: the beams at frequencies ω_1 and ω_2 interact and generate a field at the sum frequency ω_3; the generated field at ω_3 sustains a Zakharov–Manakov soliton which decays into solitons at frequencies ω_1 and ω_2 [15]. Here we report the experimental evidence of the transition from steady sum frequency generation to solitonic decay in optics. To our knowledge, this is the first experimental observation of diffractionless soliton dynamics.

2. Frequency conversion and Solitonic Decay: Theoretical Concepts

Three quasi–monochromatic waves with wave–numbers k_1 , k_2 , k_3 and frequencies ω_1 , ω_2 , ω_3, which propagate in a dispersive nonlinear medium with quadratic nonlinearity, interact efficiently with each other and exchange energy if the resonance conditions $k_1 + k_2 = k_3$, $\omega_1 + \omega_2 = \omega_3$, are satisfied. The evolution equations for the waves in a two dimensional medium,

#112662 - $15.00 USD Received 12 Jun 2009; accepted 18 Jun 2009; published 27 Jul 2009

after a multiscale expansion of Maxwell equations, turn out to be:

$$\begin{aligned}\left(\frac{\partial}{\partial z}+V_1\frac{\partial}{\partial x}\right)\phi_1 &= \eta_1 K^*\phi_2^*\phi_3,\\ \left(\frac{\partial}{\partial z}+V_2\frac{\partial}{\partial x}\right)\phi_2 &= \eta_2 K^*\phi_1^*\phi_3,\\ \left(\frac{\partial}{\partial z}+V_3\frac{\partial}{\partial x}\right)\phi_3 &= \eta_3 K\,\phi_1\phi_2.\end{aligned} \tag{1}$$

Here ϕ_n are complex wave-packet amplitudes at frequencies ω_n, V_n are characteristic velocities, η_n are signs, and K is a complex coupling coefficient. The variables x and z stand for transverse and longitudinal coordinate, respectively. Here, we consider the three–wave exchange type interaction [1], which means $(\eta_1,\eta_2,\eta_3)=(+,+,-)$ and $V_1<V_3<V_2$. It should be pointed out that the physical meaning of the waves ϕ_n, and of the variable x and z depends on the particular physical domain that one has in mind (plasma physics, nonlinear optics, fluid dynamics).

The physical model describing TWRI is completely integrable [15, 17]. The integrability of the equations (1) follows from the fact that these equations are the compatibility conditions of two 3×3 matrix Ordinary Differential Equations (ODEs), one in the variable x and the other one in z (the Zakharov–Manakov (ZM) eigenvalue problem [18]). This fact gives a way to set up a nonlinear generalization of the Fourier analysis of solutions of the associated initial value problem, namely the Inverse Scattering Technique (IST). In particular, this generalization leads to decompose a given solution $\phi_1(x,z),\phi_2(x,z),\phi_3(x,z)$ as functions of x at a given fixed z in its continuum spectrum component (radiation) and in discrete spectrum component (solitons).

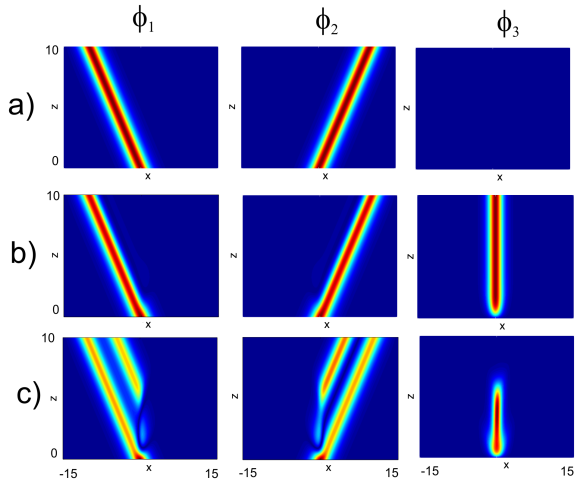

Fig. 1. Numerical $x-z$ TWRI dynamics of waves at frequency ω_1 and ω_2 which mix to generate a field at the sum frequency ω_3. (a) Linear, (b) frequency conversion, and (c) solitonic regime.

Here, we consider the TWRI dynamics of two arbitrary, almost equal and overlapping input beams at frequency ω_1 and ω_2 which mix to generate a field at the sum frequency ω_3. Depending on the input intensities, three different regimes exist, which we define as linear, frequency conversion, and solitonic regime (Fig. 1). Figure 1 shows numerical simulations, with

#112662 - $15.00 USD Received 12 Jun 2009; accepted 18 Jun 2009; published 27 Jul 2009

$V_1 = -V_2$ and $V_3 = 0$, of the typical wave dynamics in the $x-z$ plane, corresponding to the initial data at $z = 0$: $\phi_1(x,0) \neq 0$, $\phi_2(x,0) \neq 0$, $\phi_3(x,0) = 0$. In particular, figure 1.a shows the low–intensity linear regime: the beams at frequency ω_1 and ω_2 do not interact and propagate with their own characteristic velocities V_1 and V_2. Note that, from a theoretical IST perspective, the decomposition of the initial data $\phi_1(x,z=0), \phi_2(x,z=0), \phi_3(x,z=0)$ in a continuum spectrum component (radiation) and a discrete spectrum component (solitons) is irrelevant in this case since the wave–wave interaction is quite negligible. Figure 1.b shows that, at moderate input intensity, the beams at frequency ω_1 and ω_2 interact and generate a steady field at the sum frequency ω_3. When the faster wave overtakes the slower one, we observe energy conversion to the sum frequency wave ϕ_3; next the three waves propagate alone with their own characteristic velocities. In this case, the initial data $\phi_1(x,z=0), \phi_2(x,z=0), \phi_3(x,z=0)$ are composed of a continuum spectrum component (radiation) and no discrete spectrum component (solitons). Figure 1.c shows that, at relatively high input intensity, the beams at frequency ω_1 and ω_2 interact and generate a field at the sum frequency ω_3. The sum frequency wave ϕ_3 has enough energy to sustain at least one soliton. After the non–collinear nonlinear interaction the radiation parts of the waves at ω_1 and ω_2 and the wave at ω_3 propagate alone with their own characteristic velocities; furthermore, the component at ω_3 decays into two waves at ω_1 and ω_2. This decay process may be described in terms of the analytical solutions of equations (1) which were discovered in the 70*s* [15] (the ZM TWRI solitons). From a theoretical IST perspective, the initial data $\phi_1(x,z=0), \phi_2(x,z=0), \phi_3(x,z=0)$ are composed of both a continuum spectrum component (radiation) and a discrete spectrum component (solitons). Indeed the input waves ϕ_1 and ϕ_2 contain one soliton each plus radiation. The solitons in the waves ϕ_1 and ϕ_2 interact and generate a soliton in wave ϕ_3 which, due to its finite lifetime, eventually decays into solitons in the waves ϕ_1 and ϕ_2.

3. Frequency conversion and Solitonic Decay: Experiments

In order to provide the experimental demonstration of the above discussed nonlinear dynamics, we considered the optical spatial non–collinear scheme with type II second harmonic generation (SHG) in a birefringent KTP crystal. Two orthogonally polarized beams at frequency $\omega_1 = \omega_2 = \omega$, E^e_ω and E^o_ω, were injected into the nonlinear birefringent medium to cross and overlap at the input face of the crystal (see Fig. 2). Each field is linearly polarized and aligned with a polarization eigenstate of the crystal. In the present scheme the two input waves required for the parametric processes to occur, and for the subsequent observation of solitonic decay, had tilted wave–fronts. In the overlapping area the harmonic $E^e_{2\omega}$ at $\omega_3 = 2\omega$ is generated along a direction which maximized the conversion efficiency as it was fixed by the noncollinear phase–matching conditions. The sum–frequency harmonic propagation direction was found in between the directions of the two input waves.

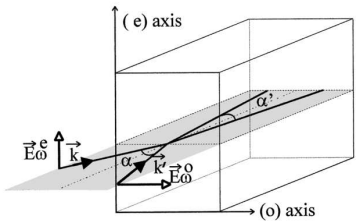

Fig. 2. Schematic representation of the optical non collinear TWRI interaction in a KTP crystal.

#112662 - $15.00 USD Received 12 Jun 2009; accepted 18 Jun 2009; published 27 Jul 2009

In details, the experiments were performed with a Q-switched, mode-locked Nd:YAG laser that delivered $40ps$ pulses at $\lambda = 1064$nm. Then laser light passed through a spatial telescope made from two lenses, L_1 and L_2. We introduced a Glan polarizer to obtain, after passage of the light through L_2, two independent beams with perpendicular linear polarization states. A half-wave plate placed before the prism served to adjust the intensity I_1 and I_2 of the two beams at an equal level I. By means of two highly reflecting mirrors, a beam splitter and a third lens L_3, both beams were focused and spatially superimposed in the plane of their beam waist with a circular shape of $120\mu m$ width (FWHMI). A $3cm$ long type II KTP crystal cut for second harmonic generation was positioned such that its input face corresponds to the plane of superposition of the two input beams. The crystal was oriented for perfect phase matching. The directions of the linear polarization state of the two beams were adjusted to coincide with the ordinary and the extraordinary axes, respectively, of the KTP crystal. The wave vectors of the input fields were tilted at angles of $\theta_1 = 0.7^o$ and $\theta_2 = -0.7^o$ (in the crystal) with respect to the direction of perfect collinear phase matching for the extraordinary and the ordinary components, respectively. These parameters corresponded inside the crystal to a tilt between the input beams equal to 3.7 times the natural walk–off angle but introduced along the ordinary noncritical plane. The sum frequency direction lies in between the input waves directions. With these values of parameters, spatial diffraction and temporal dispersion were negligible. Therefore, the dynamics of the waves could be well described by the TWRI $(1+1)$D spatial model equations (1) in the ordinary plane. The spatial waves' patterns at the output of the crystal were imaged with magnification onto a CCD camera and analyzed. We used alternately different filters and polarizers to select either the IR or the green output. As the intensities of the input fields were

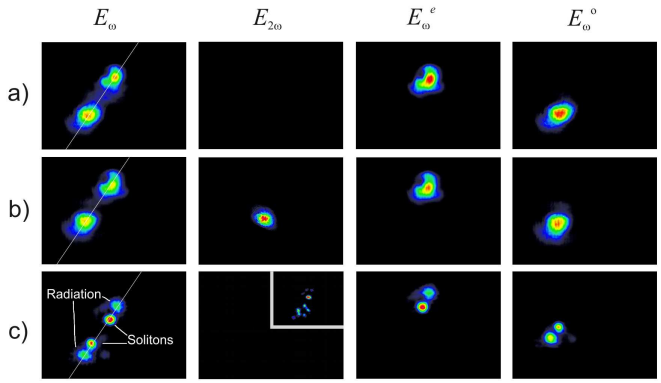

Fig. 3. Experimental results at the exit face of the KTP crystal presenting the spatial output profile of E_ω, $E_{2\omega}$, E^e_ω and E^o_ω. (a) Linear regime, $I = 1MW/cm^2$; (b) frequency conversion, $I = 0.1GW/cm^2$; (c) solitonic decay $I = 2.5GW/cm^2$. The white line in the panels labeled E_ω represents the intersection between the exit face of the crystal and the ordinary plane. The inset in panel (c) refers to the output profile of $E_{2\omega}$ without attenuation filters.

varied in a suitable range, we observed the TWRI linear, frequency conversion, and solitonic regimes in the ordinary KTP plane (Fig. 3). For each regime, Fig. 3 shows i) the output profile of the waves at frequency ω, ii) the profile of the wave at the sum frequency, iii) the profile of the extraordinary polarized component and iv) the profile of the ordinary polarized component at frequency ω. In the low–intensity ($I = 1MW/cm^2$) linear regime, the input waves did not interact and propagated without diffraction in the KTP crystal following their own characteristic directions (Fig. 3.a). The waves E^e_ω and E^o_ω, superimposed at the crystal entrance, were

#112662 - $15.00 USD Received 12 Jun 2009; accepted 18 Jun 2009; published 27 Jul 2009

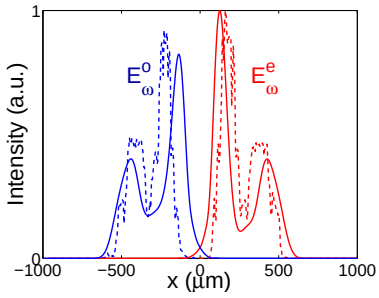

Fig. 4. Solitonic decay, $I = 2.5GW/cm^2$. Experimental (dashed lines) and numerical (solid lines) spatial output profiles at the exit face of the KTP crystal along x, intersection between the exit face of the crystal and the ordinary plane. E^e_ω (red lines), and E^o_ω (blue lines).

spatially separated at the crystal output. At moderate input intensity ($I = 0.1GW/cm^2$), parts of the beams E^e_ω and E^o_ω interacted and generated a steady field at the sum frequency. At the crystal output we observed a component of beams E^e_ω and E^o_ω which did not interact and behave linearly and the generated wave at the sum frequency $E^e_{2\omega}$ whose propagation direction lies in between the input waves directions in the ordinary plane (Fig. 3.b). This regime corresponds to the well known optical non–collinear sum frequency wave generation. At higher input intensity ($I = 2.5GW/cm^2$), we observed again the amount of the wave E^e_ω and E^o_ω which did not interact and behave as linear waves (Fig. 3.c). Moreover, we observed the birth of two well defined ordinary and extraordinary waves E^e_ω and E^o_ω, which turned out to be spatially shifted with respect to the linear components. The observation of the two new spatially shifted waves provided a clear evidence that a TWRI soliton was generated at the sum frequency within the crystal: such soliton had subsequently decayed into two solitons in the fundamentals right before the end face of the crystal. In fact, the wave at the sum frequency disappeared. Indeed, by removing the attenuation filters used to protect the camera, we may observe a faint component at the sum frequency 2ω which is generated in part through type II interaction and mainly through type I SHG by the extraordinary wave at ω (see inset of Fig. 3.c). Numerical simulations of the optical interactions, described by the equations (1), well reproduce the experimental results (see Fig. 4). The above discussed results represent the experimental evidence of the transition from a sum–frequency wave generation to a TWRI solitonic decay.

4. Conclusions

In conclusion, we have theoretically and experimentally investigated the spatial dynamics of two diffractionless beams at frequency ω_1, ω_2 which mix to generate a field at the sum frequency ω_3. Depending on the intensity, when the generated field at ω_3 can sustain a TWRI soliton, it decays into solitons at ω_1 and ω_2. Our experimental findings demonstrate the possibility of reaching soliton regimes in non-diffractive TWRI systems; these nonlinear regimes could pave the way to the construction of novel systems for storing, retrieving and processing information in the optical and plasma domains.

Acknowledgements

The present research in Brescia is supported by the MIUR project PRIN 2007–CT355C, in Rome by the University “Sapienza”.

#112662 - $15.00 USD Received 12 Jun 2009; accepted 18 Jun 2009; published 27 Jul 2009